Longitudinal laser ion acceleration in gas jets: experimental optimization on the Titan laser facility and numerical investigation of the ultra-high intensity limit

E. d'Humières[1], S. Chen[2], P. Antici[3], M. Bailly-Grandvaux[1], T. Gangolf[2], M. Lobet[4], G. Revet[2], A.M. Schroer[5], O. Willi[5], J. Santos[1], V. Tikhonchuk[1], H. Pépin[3], J. Fuchs[2]

[1]*Univ. Bordeaux, CNRS, CEA, CELIA, UMR 5107,33400 Talence, France*

[2]*LULI, École Polytechnique, CNRS, CEA, UPMC, route de Saclay, 91128 Palaiseau, France*

[3]*INRS-ENT, Varennes, Québec, Canada*

[4]*CEA, DAM, DIF, 91297 Arpajon, France*

[5]*Institut für Laser-und Plasmaphysik Heinrich Heine Universität Düsseldorf*

Intense research is being conducted on sources of laser-accelerated ions and their applications [1]. Several experiments on the low density regime of laser ion acceleration [2] were performed in recent years. In this regime, volume effects are expected to dominate, while for solid foils, ion acceleration is directly related to the electron surface density and the number of accelerated ions is limited. Simulations therefore show that it is possible to reach high ion energies with a high number of accelerated ions and a high conversion efficiency [3]. This scheme also leads to less debris than solid foils and is more adapted to high repetition lasers.

Very promising results were recently obtained at LULI [4] and on the LLNL Titan laser in this regime [5]. In both experiments, a first ns pulse was focused on a thin target to explode it and a second laser with a high intensity was focused on the exploded foil. The delay between two lasers allowed to control the density gradient seen by the second laser pulse. The transition between various laser ion acceleration regimes depending on the density gradient length was studied. With a laser energy of a few Joules, protons with energies close to the energies of TNSA accelerated protons were obtained for various exploded foils configurations. In the high energy regime (~180 J), protons with energies significantly higher than the ones of TNSA accelerated protons were obtained when exploding the foil while keeping a good beam quality. These results demonstrate that low-density targets are promising candidates for an efficient proton source that can be optimized by choosing appropriate plasma conditions.

We report on new experiments performed on the Titan laser in 2014 using compact and dense gas jets made available recently by important progresses on nozzle optimization [6]. The experimental optimization of longitudinal laser ion acceleration is discussed using this setup, which is very promising for several applications of laser ion acceleration even if important progresses are still required on the maximum energy of the beam.

The Titan short pulse with a 0.7 ps duration, a wavelength of 1054 nm, a 26 microns FWHM was focused on a hydrogen gas jet with a characteristic full width at half maximum of 300 microns on the propagation axis. The laser energy was varied from 50 to 180 J (corresponding to laser intensities up to $7x10^{19}$ W/cm^2). By varying the pressure from 180 bars to 900 bars, the maximum density of the gas jet ranged from 0.5 n_c to 2.5 n_c. Three Thomson Parabolas at 0°, 16° and 32° from the short pulse propagation axis were used as well as a proton spectrometer at 90°. Depending on the maximum density of the gas jet, pure highly collimated proton beams with quasi-monoenergetic structures were measured for the first time at this wavelength.

Preliminary 1D Particle-In-Cell simulations were performed with the code PICLS [7]. The laser parameters are the same as above and the density profile corresponds to a lineout of the density measured in the experimental configuration. Proton energy spectra measured in the increasing part of the density gradient after 4 ps for two laser intensities are plotted in Figure 1. A peaked structure, similar to the one observed in the Titan experiments, is visible between 2 and 4 MeV in both cases. An analysis of the phase spaces shows that this structure corresponds to the electrostatic shock launched in the increasing gradient by the laser pulse.

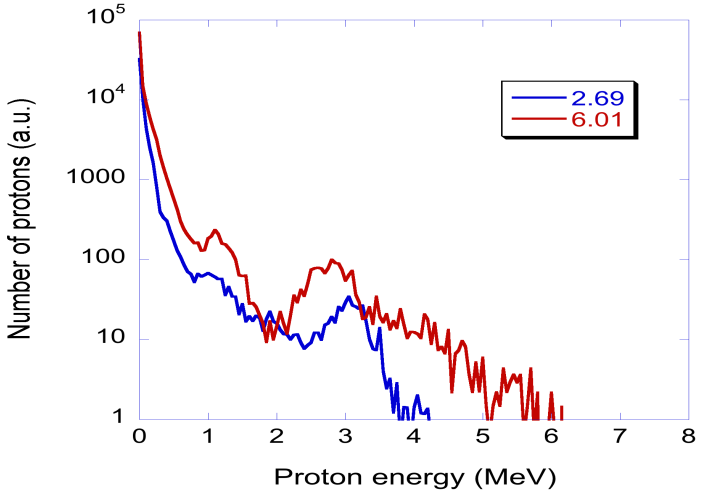

Figure 1: Proton energy spectra measured in the increasing part of the density gradient after 4 ps for a_0=2.69 (blue line) and for a_0=6.01 (red line).

Scaling shock acceleration in the low density regime to ultra high intensities (>10^{22} W/cm^2) is a challenge as radiation losses and electron positron pair production change the optimization of the shock process. Using large-scale Particle-In-Cell simulations including these effects, we have investigated and modeled the transition to this regime in which intense beams of relativistic ions can be produced.

Following Refs. [8,9], the PIC code CALDER [10] has been enriched with numerical models of synchrotron radiation and Breit-Wheeler pair production [11]. In the classical case, the low-energy photon emission is treated using Sokolov's radiation friction model with a quantum-corrected radiated power [12]. In the quantum regime, Monte Carlo schemes are used to describe the discrete emission of gamma photons and their annihilation into e–e+ pairs. The physical parameters are chosen so as to reproduce laser and target conditions that could be tested with near-future laser installations like Apollon in France and the Extreme Light Infrastructure in Europe. The linearly-polarized laser pulse has a 1 μm wavelength, a 32 fs (60 ω_0^{-1}, where ω_0 is the laser frequency) FWHM duration and a peak intensity ranging from $I_0 = 10^{22}$ to 8.9×10^{23} Wcm^{-2} (i.e., a normalized field amplitude $a_0 = eE_0/m_e c\omega_0 = 85$ to 800). The focal spot FWHM is 10 μm. The target is taken to be a fully-ionized H plasma with a cosine squared density profile, a maximum electron density $n_e = 2\ n_c$ and a total thickness ranging from 100 to 400 μm.

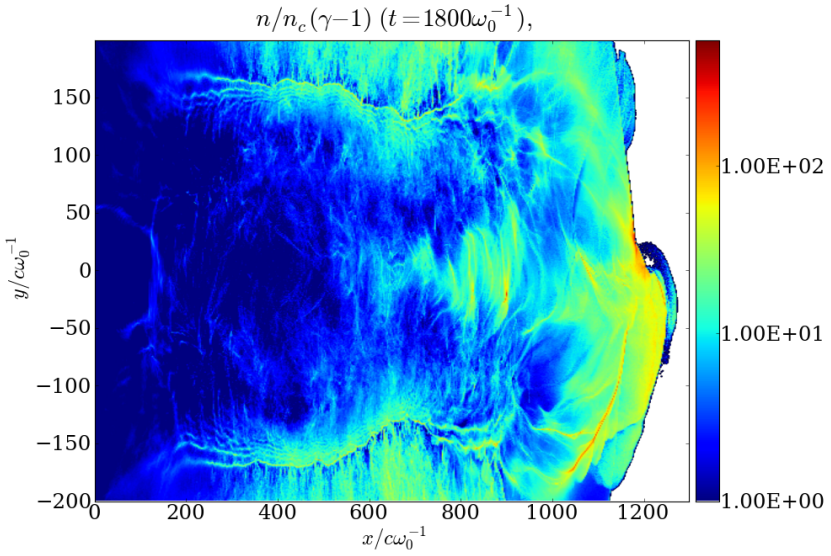

Figure 2: 2D map of the proton energy density after 1800 ω_0^{-1} for I=10^{22} W/cm^2 for a 2 n_c, 150 microns long cos^2 target. The laser comes from the left side of the simulation box.

Figure 2 shows the 2D map of the proton energy density after 1800 ω_0^{-1} for I=10^{22} W/cm^2 for a 2

n_c, 150 microns long $\cos^2$ target. As already described in [5], the high concentration of ion energy density and the complexity of the high energy ion front which is followed by high energy filamentary structures is clearly visible. Proton energies of more than 900 MeV are measured in these simulations.

In summary very promising results were recently obtained in the low density regime of laser ion acceleration using new nozzles able to deliver denser and more compact gas jets. The experimental optimization of longitudinal laser ion acceleration can be achieved using this setup, which is very promising for several applications of laser ion acceleration even if important progresses are still required on the maximum energy of the beam.
Using large-scale Particle-In-Cell simulations including these effects, we have investigated and modeled the transition to the ultra high intensity regime of laser ion acceleration in low density targets in which intense beams of relativistic ions can be produced. These relativistic ion beams are of great interest for high-energy laboratory astrophysics.

[1] A. Macchi et al., Rev. Mod. Phys. 85, 751 (2013); E. d'Humières (2012). Ion Acceleration by High Intensity Short Pulse Lasers, Laser Pulses - Theory, Technology, and Applications, Prof. Igor Peshko (Ed.), ISBN: 978-953-51-0796-5, InTech, DOI: 10.5772/46137.
[2] L. Willingale et al. Phys. Rev. Lett. 96, 245002 (2006); P. Antici et al. New J. Phys. 11, 023038 (2009); C. Palmer et al., Phys. Rev. Lett. 106, 014801 (2011); D. Harberger et al., Nature Physics 8, 95 (2012).
[3] E. d'Humières et al., J. Phys.: Conf. Ser. 244, 042023 (2010); F. Fiuza et al. Phys. Rev. Lett. 109, 215001 (2012); E. d'Humières et al., Phys. Plasmas 20, 023103 (2013).
[4] M. Gauthier et al. Phys. Plasmas 21, 013102 (2014).
[5] E. d'Humières, et al., Plasma Phys. Controlled Fusion 55, 124025 (2013).
[6] F. Sylla et al., Rev. of Sci. Inst. 83, 033507 (2012); S.N. Chen et al., Nuclear Instruments and Methods in Physics Research Section A: Accelerators, Spectrometers, Detectors and Associated Equipment 740, 105-106 (2014).
[7] Y. Sentoku, E. d'Humières, L. Romagnani, P. Audebert, J. Fuchs, Phys. Rev. Lett. 107, 135005 (2011).
[8] R. Duclous R., J.G. Kirk, and A.R. Bell, Plasma Phys. Control. Fus., 53, 015009 (2011).
[9] N.V. Elkina, A.M. Fedotov, I.Y. Kostyukov, et al., Phys. Rev. ST Accel. Beams 14, 054401 (2011).
[10] E. Lefebvre et al., Nuclear Fusion 43, 629 (2003).
[11] M. Lobet, E. d'Humières, M. Grech, et al., arXiv preprint arXiv:1311.1107 (2013).
[12] I.V. Sokolov, N.M. Naumova, J.A. Nees, et al., Phys. Plasmas 16, 093115 (2009).